Probabilistic Seismic Analyses of Earthen Levees with Finite Element Modeling

Liang Zhang[1]; Weiwei Zhan[2]; Lei Wang[3*]

[1]Research Assistant, Department of Civil and Architectural Engineering and Construction Management, University of Cincinnati, Cincinnati, OH 45221, USA. Email: zhang4lg@mail.uc.edu

[2]Post-Doctoral Fellow, Department of Civil and Environmental Engineering, Tufts University, Medford, MA, 02155, USA. Email: weiwei.zhan@tufts.edu

[3]Assistant Professor, Department of Civil and Architectural Engineering and Construction Management, University of Cincinnati, Cincinnati, OH 45221, USA. Email: wang4li@ucmail.uc.edu (corresponding author)

Abstract: Earthen levees are critical civil infrastructure of coastal regions for flood protection. Earthquake can cause significant deformation and damage to earthen levees. Seismic performance of such levees under the earthquake hazards is a major concern in their safety evaluation. However, there are significant uncertainties in assessing the seismic behavior of earthen levees and geotechnical uncertainties play a critical role in the probabilistic assessment of earthquake-induced deformation and failures. This paper presents a simplified probabilistic framework for assessing the seismic performance of earthen levees with dynamic analysis and finite element modeling. In this framework, the effects of geotechnical uncertainties are explicitly considered in the uncertainty propagation for probabilistic evaluation of seismic deformations of earthen levees under earthquake hazards. The probability curves are developed to describe the correlations among the probability of exceedance, limiting deformation value, and input peak ground acceleration. The derived probability curves can provide valuable information for risk assessment and risk-informed decision-making of earthen levee infrastructure. The effectiveness of the proposed probabilistic framework is demonstrated through a case study of earthen levee example.

Keywords: Displacement; Earthen Levee; Earthquake; Finite Element Method; Uncertainty.

Introduction

Earthen levees are critical civil infrastructure protecting coastal regions for flood hazards due to various drives such as coastal water level, precipitation, and river discharge (Jasim et al. 2020). It is estimated that there are over 100,000 miles of levees in the United States (Zevenbergen et al. 2017). Many of the levees have lived out their design life, and some are over 100 years old. The safety evaluation of the earthen levees under hazard conditions is a major concern to prepare the infrastructure for the disaster resilience, especially for those located in the seismically active zone. For example, the levee system in the Sacramento-San Joaquin Delta, which protects one of the most at-risk regions in the United States for catastrophic flooding, is also highly susceptible to earthquake-induced damage and failure. Thus, it is critical to evaluate the reliability of earthen levees in the face of earthquake hazards since the failure of such structures can be catastrophic and cause loss of lives, damage to properties, and significant adverse economic and societal impacts.

The earthquake-induced deformation and damages to earthen levees due to expected ground shaking levels are difficult to predict due to a variety of factors, and geotechnical variability is an important contributing factor to the variability of earthquake-induced deformations. The stability and performance of the slopes and levees have been investigated by many researchers using deterministic methods including pseudo-static analysis, permanent-displacement analysis, and stress-deformation analysis (Newmark 1965; Sarma et al. 1975; Makdisi and Seed 1978; Rathje and Bray 2000; Jibson 2011; Stark et al. 2012; Wang et al. 2021). Among these methods, stress-deformation analysis can utilize dynamic methods such as dynamic finite element and finite difference methods to incorporate sophisticated soil-constitutive models in evaluating the stress-strain behavior of soil slopes (Jibson 2011). However, in such analysis, significant uncertainties exist in the modeling of the dynamic soil behavior due to limited site investigation and difficulties to obtain high-quality samples for soil testing. Many existing probabilistic studies on the earthen levees and embankments focus on static analyses or using pseudo static methods in seismic analyses (Duncan 2000; Xiao et al. 2016; Wang et al. 2020; Zhang et al. 2022). In addition, when the seismic performance of levees is evaluated using stress-deformation analysis implemented in a numerical model without an explicit solution, the computational efforts of probabilistic seismic analyses could be challenging (Zhang et al. 2013). This paper aims to: 1) establish dynamic finite element models for evaluating the seismic performance of earthen levees; 2) develop a probabilistic framework to explicitly consider the geotechnical uncertainties through the combined advanced reliability assessment and numerical methods; 3) demonstrate the efficiency and effectiveness of the proposed methods with a case study for earthen levees. The probabilistic framework is formulated using an efficient reliability method that accounts for the propagation of uncertainties from the input random variables through the dynamic finite element modeling. The derived probability curves can provide useful references for more informed decision-making for the stakeholders in risk management of levees. A case study is utilized to demonstrate the effectiveness of the proposed probabilistic framework in assessing the seismic performance of earthen levees.

Dynamic Analysis of Earthen Levees

Finite element method (FEM) and finite difference method (FDM) are widely employed in predicting the performance of earthen levees under earthquake loads. These methods involve dividing the entire model domain into deformable sub-domains and calculating the stress and strain at the connected nodes. The dynamic analysis implemented in the finite element method, namely the dynamic finite element method, is employed in this study, which can accurately simulate complex geological conditions and soil behaviors under dynamic loads. The dynamic finite element method enables seismic geotechnical analyses of the propagation of waves through the soil and their impacts on geotechnical structures. The ground motion data will be used to evaluate the levee's seismic response, which can determine the deformation characteristics of the levee over the time history. The numerical model for analyzing the earthen levee performance is built using the finite element program PLAXIS 2D under the plane-strain condition. In the dynamic analysis, the Hardening Soil Model with Small Strain Stiffness (HS Small) is utilized for modeling the soil behavior. The model is a built-in constitutive model in PLAXIS 2D for seismic geotechnical analyses. The HS Small model can capture the nonlinear and inelastic stress-strain behavior of both stiff and soft soils, especially for the nonlinear stiffness decay at the small strain levels. The hysteretic damping subjected to cyclic shear loading is also considered in the HS Small model (Brinkgreve et al. 2007). Compared with the classic hardening soil model, two additional parameters are used to model the variation of stiffness with strain, including the initial shear modulus G_0 and the shear strain level at which the secant shear modulus G_s is reduced to approximately 70% of G_0 (Brinkgreve et al. 2017). In the dynamic finite element analysis, since the dynamic motion is applied to the base of soil deposits, a compliant base boundary condition is applied at the bottom boundary and free-field boundary conditions are applied at the lateral boundary of the model (e.g., the left and right sides of the model as shown in Figure 1). The fine mesh is used for modeling with enhanced mesh refinement at the embankment section.

Probabilistic Framework for Seismic Performance of Earthen Levees

Here a probabilistic framework for seismic performance of levees is developed by combining the advanced reliability theory and the dynamic finite element modeling. In this paper, the deformation characteristics of levees under various earthquake hazard levels in terms of peak ground acceleration will be assessed using a quantitative probabilistic assessment framework. The probabilistic framework includes four steps as follows: 1) uncertainty characterization of input parameters for the dynamic analyses; 2) establishment of a deterministic numerical model; 3) uncertainty propagation using advanced moment methods combined with point estimate method (PEM); 4) derivation of probabilistic curves for decision-making.

The probability of levee damage under the given earthquake hazard can be evaluated using the probability of exceedance, which is the probability that the predicted maximum displacement of the levee ($D_{\max}$) exceeds a given limiting displacement threshold value ($D_{\lim}$). The maximum permanent displacement of the earthen levee is evaluated using the dynamic finite element method. Then the performance function, denoted as G, for determining the probability of exceedance can be written as:

$$G = D_{\lim} - D_{\max} \tag{1}$$

where the levee is safe if the obtained performance function G is greater than 0 (i.e., $D_{\lim} > D_{\max}$).

The probability of exceedance can be determined using an advanced point estimate method (PEM). Here the PEM method uses selected five points sampled from the probability distribution function to estimate the four moments of the performance function, namely the mean, standard deviation, skewness, and kurtosis. The accuracy of the advanced point estimate method has been demonstrated with many engineering examples (Zhao and Ono 2000&2001).

In the PEM procedure, the estimating points are obtained from the space of standard normal distribution. For other probability distributions, the Rossenblatt transformation can be used to transform estimating points in the original space (x_j) into the counterparts in the standard normal space (u_j). The Hermite integration can then be used to obtain the estimated points and their corresponding weights in the standard normal space, which can be used to evaluate the k^{th} central moment of a function in the original space, $y= y(x)$ using the following equation (Zhao and Ono 2000):

$$\mu_y = \sum_{j=1}^{m} P_j y[T^{-1}(u_j)] \tag{2}$$

$$M_{ky} = \sum_{j=1}^{m} P_j (y[T^{-1}(u_j)] - \mu_y)^k \tag{3}$$

where μ_y is the mean value, M_{ky} is k^{th} dimensionless central moment of $y(x)$, T^{-1} is the inverse Rosenblatt transformation. $u_1, u_2, u_3, \ldots, u_m$ are the estimating points and $P_1, P_2, \ldots, P_m$ are the corresponding weights.

For the levee problem with multiple uncertain parameters as input random variables (assuming N uncertain input parameters for illustration purpose), and the performance function can be written as $G = G(\boldsymbol{Z}) = G(Z_1, Z_2, Z_3,\ldots, Z_N) = D_{lim} - D_{max} (Z_1, Z_2, Z_3,\ldots, Z_N)$, where $G(\boldsymbol{Z})$ is the performance of the levee for evaluating the probability of exceedance. Since there is no explicit solution for evaluating the seismic performance, the PLAXIS 2D model is treated as the implicit performance function in the proposed probabilistic framework. The performance function is a function of all the uncertain input parameters, which will be evaluated based on the uncertainty propagation through the dynamic finite element modeling to obtain D_{max} under the given earthquake loading.

The four moments of $G = G(\boldsymbol{Z}) = G(Z_1, Z_2, Z_3,\ldots, Z_N)$ can be evaluated following the below equations:

$$\mu_G = (\mu_1 - G_\mu) + (\mu_2 - G_\mu) + \ldots + (\mu_N - G_\mu) + G_\mu \tag{4}$$

$$\sigma_G^2 = \sigma_1^2 + \sigma_2^2 + \ldots + \sigma_N^2 \quad (5)$$

$$\alpha_{3G}\sigma_G^3 = \alpha_{31}\sigma_1^3 + \alpha_{32}\sigma_2^3 + \ldots + \alpha_{3N}\sigma_N^3 \quad (6)$$

$$\alpha_{4G}\sigma_G^4 = \alpha_{41}\sigma_1^4 + \alpha_{42}\sigma_2^4 + \ldots + \alpha_{4N}\sigma_N^4 + 6\sum_{i=1}^{N-1}\sum_{j>1}^{N}\sigma_i^2\sigma_j^2 \quad (7)$$

where G_μ is the performance function $G(Z_1, Z_2, Z_3, \ldots, Z_N)$ evaluated at the mean of input random variables (Z_1, Z_2, $Z_3, \ldots, Z_N$); μ_1, σ_1, α_{31}, α_{41} are the mean, standard deviation, skewness coefficient and kurtosis coefficient of $G(Z_1, Z_2 = \mu_2, Z_3 = \mu_3, \ldots, Z_N = \mu_N)$ evaluated with only one random variable Z_1 using Eq. (2) and Eq. (3). μ_2, σ_2, α_{32}, α_{42}, μ_3, σ_3, α_{33}, α_{43} and μ_N, σ_N, α_{3N}, α_{4N} can be evaluated using the similar procedures. Based on the above results, the four moments of the performance function of the earthen levee problem can then be evaluated using Eqs. (4-7). By correlating the probability of exceedance with central moments using different formulations (Zhao and Ono 2001; Ang and Tang 2007), the moment methods can be employed to assess the probability of exceedance for the given earthquake load (e.g., in term of peak ground acceleration). Three moments methods, namely, Second moment (SM) method, Third Moment (TM) method, and Fourth Moment (FM) method are described. The main difference of three moments methods lies in their difference in the approximation of the distribution of the performance function using different orders of the moment. The third moment method can consider asymmetric random variables by introducing a three-parameter lognormal distribution, and a higher-order moments standardization technique (HOMST) is utilized in the fourth moment formulation (Zhao and Ono 2001).

The second moment method has the same basic principle with the First-order second moment method (Ang and Tang 2007). The following equation can be used to evaluate the reliability index and probability of exceedance:

$$\beta_{SM} = \frac{\mu_G}{\sigma_G} \tag{8}$$

$$P_{E-SM} = \Phi(-\beta_{SM}) \tag{9}$$

where μ_G and σ_G are the mean and standard deviation of $G = G(\mathbf{Z})$, respectively; $\Phi(\bullet)$ is the standard normal cumulative distribution function.

For the third moment method, the standardized variable of the performance function $G = G(\boldsymbol{Z})$ is considered to follow the three-parameter lognormal distribution (Tichy 1994):

$$Z_u = \frac{Z - \mu_G}{\sigma_G} \tag{10}$$

The intermediate variable in terms of a standard normal random variable u, for evaluation of reliability index, is expressed as a function of first three moments of the performance function as (Tichy 1994; Zhao and Ono 2001):

$$u = \frac{sign(\alpha_{3G})}{\sqrt{\ln(A)}} \ln\left[\sqrt{A}\left(1 - \frac{Z_u}{u_b}\right)\right] \tag{11}$$

where A and u_b are functions of α_{3G} based on formulations documented in Zhao and Ono (2001).

Following the formulation of third moment method (Tichy 1994), the reliability index and probability of exceedance are determined as:

$$\beta_{TM} = \frac{-sign(\alpha_{3G})}{\sqrt{\ln(A)}} \ln\left[\sqrt{A}\left(1 + \frac{\beta_{SM}}{u_b}\right)\right] \tag{12}$$

$$P_{E-TM} = \Phi(-\beta_{TM}) \tag{13}$$

The fourth moment method is built upon the principle of high-order moment standardization (Ono and Idota 1986), the standard normal variable can be expressed using the following equation (Zhao and Ono 2001):

$$u = \frac{\alpha_{3G} + 3(\alpha_{4G} - 1)z_u \text{-} \alpha_{3G} z_u^2}{\sqrt{(5\alpha_{3G}^2 - 9\alpha_{4G} + 9)(1 - \alpha_{4G})}} \tag{14}$$

The reliability index and probability of exceedance can be evaluated using the formulation documented by Ono and Idota (1986) as:

$$\beta_{FM} = \frac{3(\alpha_{4G} - 1)\beta_{SM} + \alpha_{3G}(\beta_{SM}^2 - 1)}{\sqrt{(9\alpha_{4G} - 5\alpha_{3G}^2 - 9)(\alpha_{4G} - 1)}} \tag{15}$$

$$P_{E-FM} = \Phi(-\beta_{FM}) \tag{16}$$

Example Application

This section uses a case study of an existing earthen levee to demonstrate the probabilistic seismic assessment framework. The studied levee is adapted from a real levee built in 1990s for flood protection, which runs along a parking lot holding back a substantial area including wetlands. The earthen levee is built on top of a permanent soil foundation and composed of three types of geotechnical materials (i.e., embankment soil, rockfill zone, and No. 57 stone). The representative cross section of the levee is shown in Figure 1. The widths of the levee base and crown are 16.4 m and 0.3 m, respectively. The height of the levee is 3.35 m, and both sides of the levee have a slope ratio of 2:1 (horizontal to vertical). The rockfill zone has a base width of 6.7 m and a height of 2.1 m. The water level is 2.1 m above the ground level, which corresponds to a flood hazard of a 100-year returning period. The groundwater table of the downstream side is 0.6 m below the ground level according to subsurface exploration results. A total of eight borings were drilled at the crown and toe of representative levee sections to estimated depths of 6 to 9 m. Nine undisturbed soil samples (Shelby tube samples) were obtained, and disturbed soil samples (split-spoon samples) were taken at regular intervals. Twenty-four sieve analysis and Atterberg limits tests were performed for selected disturbed soil samples. Two direct shear tests and one consolidation test were performed for selected undisturbed soil samples. The results from field exploration and laboratory testing are used to estimate the strength parameters of soils and the geotechnical parameters for each layer of the earthen levee used in the analysis are listed in Table 1.

Finite element modeling for the seismic performance of earthen levee

Firstly, a deterministic analysis using the dynamic finite element modeling is performed to assess the seismic performance of the earthen levee. Since the earthen levee of concern is a long linear infrastructure, it can be well analyzed using 2D finite element modeling in a plane strain configuration. Constitutive behaviors of each soil layer are modeled using the HS small model with corresponding soil parameters listed in Table 1. The earthquake loading is applied to the bottom boundary of the model. The input ground motion is obtained from the 1990 M_w 5.7 Upland Earthquake in California, USA. It is a left-lateral strike-slip earthquake that occurred west of the San Andreas Fault Systema with a maximum Mercalli Intensity of VII. The input ground motion is the North-South component of the ground motions recorded during the 1990 Upland Earthquake. The peak ground acceleration (PGA) of the input ground motion is 0.24 g. The acceleration time history of the input ground motion and its Fourier amplitude spectrum are shown in Figures 2 and 3, respectively. In the dynamic analysis, the input ground motion is applied to the base of the FEM model, which is taken from rock outcropping motion.

One of the main concerns in the seismic assessment of earthen levees is to evaluate the damage levels based on the permanent deformation, which is related to the crack and subsidence of the levee (Kwak et al. 2016). In this paper, the maximum permanent total displacement from the dynamic finite element modeling is used as a performance indicator to evaluate the probability of damage due to the earthquake load. Allowable permanent displacement is decided by damage levels of levee structures under different permanent displacements. For example, a limiting displacement value of 10 cm is typically used for classification between slight damage and moderate damage, while a limiting displacement value of 30-50 cm is typically used to distinguish between moderate damage and severe damage. A displacement of more than 100 cm generally indicates the levee collapse. The limiting deformation values are adapted from the study by Kwak et al. (2016) based on the post-earthquake reports for the levee segments throughout the Shinano River System.

Figure 4 shows the contour map of the permanent displacement of the levee, which is residual displacement at the end of the shaking. The land side of the earthen levee has a larger displacement than the flooding side. The maximum deformation contour passes through the crest to the toe of the levee in the land side. The maximum permanent displacement is 7.9 cm, which occurs around the top of the land side.

Five measurement points (i.e., the levee top-left, levee top-right, levee bottom-left, levee bottom-right, and middle-bottom points) are selected to monitor the time history of seismic response of the levee under the earthquake impacts (see Figure 1). The time histories of horizontal (X-direction) acceleration, velocity, and displacement of the five measurement points are shown in Figures 5-7, respectively. Figure 5 shows that the levee’s top-left and top-right points generally have the highest horizontal peak acceleration. A similar trend is also observed for the horizontal peak velocity as shown in Figure 6. However, the horizontal velocity tends to converge at the end of the time history compared with the horizontal acceleration. The maximum transient velocity of the levee is 0.233 m/s occurs at 2.8 s located on the top-right of the levee.

The maximum transient horizontal displacement of the levee is 0.138 m occurs at 7.2 s located on the bottom-left of the levee, and the maximum permanent (residual) horizontal displacement of the levee is 0.068 m located on the bottom-left of the levee. The resulting time history profile of horizontal displacement also indicates a larger deformation on the land side.

Probabilistic seismic assessment of earthen levee

In this section, the probabilistic seismic assessment of the example earthen levee is conducted by evaluating the probability of exceedance, which is in terms of the probability of exceeding an allowable permanent displacement value. In the probabilistic assessment, uncertainties in the strength and permeability parameters of each material layers of the levee are considered. The mean values of the soil parameters of each layer adopt the values reported in Table 1 and the coefficient of variation of these parameters are estimated based on the published literature (e.g., Phoon and Kulhawy 1999; Luo and Hu 2018; Wang et al. 2018). The statistics of uncertain soil parameters used in the probabilistic analyses are listed in Table 2 and it should be noted that the coefficient of variation (COV) of the permeability coefficient represents the COV of the permeability coefficient in its logarithmic form. The uncertainties in these parameters are propagated into the dynamic finite element modeling through the moments method formulation in evaluating the probability of exceedance.

In the evaluating of the probability of exceedance, a limiting displacement value needs to be specified, which is related to the desired performance of the levee under the given earthquake load. For demonstration purpose, a limiting permanent displacement value of 30 cm is used in the evaluation of the probability of exceedance. Using any of the moment method, the probability of exceedance evaluated under the given ground motion (PGA = 0.24 g) for a limiting displacement of 30 cm is 13.4%. Repeating this process with each of a series of limiting displacement values ranged between 5 cm to 100 cm, a probability of exceedance curve for this levee under the given ground motion is obtained, as shown in Figure 8. As can be found from Figure 8, the second moment (SM) method, third moment (TM) method, and fourth moment (FM) method generally yield similar results for the calculated probability of exceedance. For demonstration purposes, all the afterward probability of exceedance evaluations adopt the third moment method. It can be found that the probability of exceedance generally decreases with the increase in the limiting displacement values, which is expected since the less stringent performance requirement will reduce the probability of violating that requirement. The probability of exceedance curve under the given ground motion can provide a useful reference to evaluate the damage potential based on different limiting displacement values. The probability of exceedance under different limiting values can be readily obtained using Figure 8 to assess the probability in terms of different damage levels. For example, from Figure 8, it is found that the levee has a considerable probability of exceedance for a limiting displacement of 10 cm, which indicates a good possibility for slight damage. The probability of exceedance for a limiting displacement of 100 cm, which indicates levee collapse, is almost negligible.

PGA Effects on probability of exceedance curves

To evaluate the PGA effects on the probability of exceedance curves, we scale the acceleration time history in Figure 2 to different PGA values, and repeat the probabilistic analyses in the previous section using scaled input ground motions. The probability of exceedance curves under different PGA levels are shown in Figure 9. Under all three PGA levels, the probability of exceedance generally decreases with the increase in the limiting displacement value. It can be found that under the peak ground acceleration of 0.1 g, the probability of exceedance is less than 10% even with very stringent limiting displacement requirements (e.g., 5 cm) and the probability of exceedance becomes negligible after 10 cm. However, when the peak ground acceleration is 0.6 g, the probability of exceedance for a limiting displacement of 10 cm is 87%, which indicates a very high likelihood of slight damage when a displacement exceeding 10 cm is treated as the criteria for slight damage. Under the peak ground acceleration of 0.6 g, the probability of exceedance for a limiting displacement of 100 cm is about 5.8%, which suggests there could be about 5.8% chance for levee collapse under the high earthquake load when a displacement exceeding 100 cm is treated as the criteria for levee collapse.

Effect of different limiting displacement values on the probability of exceedance

In this paper, the susceptibility of the levee with regard to earthquake loads is expressed using the probability of exceedance versus the peak ground acceleration for the given limiting displacement value. Taking a limiting displacement value of 10 cm as an example, the probability of exceedance is evaluated at different peak ground acceleration levels and the resulting curve is illustrated in Figure 10. It can be found that the probability of exceedance steadily increases with the increase of the peak ground acceleration. However, the rate of increase is gradually reducing. Similar trends are also observed for the limiting displacement of 30 cm, 50 cm, and 100 cm, respectively. The levee is very susceptible to slight damage with the increase of the earthquake load. However, it generally becomes less susceptible to the relaxed damage criteria (e.g., an increase in the limiting displacement value). For example, the probability of exceedance for 100 cm (indicating collapse) is less than 10% even under the high earthquake load. The results in Figure 10 can provide useful guidance for the decision makers to consider the susceptibility of the levee with regard to earthquake loads under different damage criteria.

Concluding Remarks

This paper presents a probabilistic seismic assessment of the earthen levees using the finite element method and advanced moment method formulations. A deterministic dynamic finite element analysis of the earthen levee is first conducted based on the ground motions recorded during the 1990 Upland Earthquake in California. The resulting time histories of acceleration, velocity and displacement of represented locations are evaluated, and it is found that the maximum permanent displacement of the levee occurs in the land side of the levee. The results from the deterministic assessment are used as the basis for the probabilistic assessment. In the probabilistic assessment, the uncertainties in the geotechnical parameters are propagated through finite element simulations and the probability of exceedance curve can be readily derived to depict the relationship between the probability of exceedance with the limiting displacement value, in which different limiting displacement values correspond to different damage levels. The effects of different peak ground accelerations on the derived probability of exceedance curves are also obtained. Furthermore, the susceptibility of the levee with regard to earthquake loads is developed by expressing the probability of exceedance with respect to the increasing peak ground acceleration for the given limiting displacement requirement. It can be found that the probability of exceedance steadily increases with the increase of the peak ground acceleration for different limiting displacement values, and the results can help guide the evaluation of the susceptibility of the levee with regard to incremental earthquake loads. The effectiveness of the proposed approach is demonstrated with a case study of seismic assessment of earthen levee. The proposed approach has the potential as a practical tool for seismic assessment and allows engineers to make more informed risk-based decisions in the face of earthquake hazards.

ACKNOWLEDGMENTS

The third author wishes to acknowledge the support from the National Science Foundation through Grants 1818649 and 1900445. The results and opinions expressed in this paper do not necessarily reflect the views and policies of the National Science Foundation.

CONFLICT OF INTERESTS

The authors declare that they have no known competing financial interests or personal relationships that could have appeared to influence the work reported in this paper.

References

Ang, A.H.S., and Tang, W.H. (2007). Probability Concepts in Engineering: Emphasis on Applications to Civil and Environmental Engineering, 2nd edition, Wiley, New York.

Brinkgreve, R.B.J., Kappert, M.H., and Bonnier, P.G. (2007). Hysteretic damping in a small-strain stiffness model. Proceedings of Numerical Models in Geomechanics, NUMOG X, Rhodes, pp. 737-742, Taylor & Francis Group, London.

Brinkgreve, R.B.J., Kumarswamy, S., and Swolfs, W.M. (2017). Plaxis 2D Manual. PLAXIS bv, The Netherlands.

Duncan, J.M. (2000). Factors of safety and reliability in geotechnical engineering. Journal of Geotechnical and Geoenvironmental Engineering, 126(4), 307-316.

Jasim, F. H., Vahedifard, F., Alborzi, A., Moftakhari, H., and Aghakouchak, A. (2020). Effect of compound flooding on performance of earthen levees. In Geo-Congress 2020: Engineering, Monitoring, and Management of Geotechnical Infrastructure, Geotechnical Special Publication No. 316, pp 707-716.

Jibson, R.W. (2011). Methods for assessing the stability of slopes during earthquakes—A retrospective. Engineering Geology, 122(1-2), 43-50.

Kwak, D.Y., Stewart, J.P., Brandenberg, S.J., and Mikami, A. (2016). Characterization of seismic levee fragility using field performance data. Earthquake Spectra, 32(1), 193-215.

Luo, Z., and Hu, B. (2018). Reliability-based assessment and design of stone-filled crib seawalls for shoreline protection. Marine Georesources & Geotechnology, 36(8), 918-930.

Makdisi, F.I., and Seed, H.B. (1978). Simplified procedure for estimating dam and embankment earthquake-induced deformations. Journal of the Geotechnical Engineering Division, 104(7), 849-867.

Newmark, N.M. (1965). Effects of earthquakes on dams and embankments. Géotechnique, 15(2), 139-160.

Ono, T., and Idota, H. (1986). Development of high-order moment standardization method into structural design and its efficiency. Journal of Structural and Construction Engineering, 365, 40-47.

Phoon, K.K., and Kulhawy, F.H. (1999). Characterization of geotechnical variability. Canadian Geotechnical Journal, 36(4), 612-624.

Rathje, E.M., and Bray, J.D. (2000). Nonlinear coupled seismic sliding analysis of earth structures. Journal of Geotechnical and Geoenvironmental Engineering, 126(11), 1002-1014.

Sarma, S.K. (1975). Seismic stability of earth dams and embankments. Géotechnique, 25(4), 743-761.

Stark, T.D., Beaty, M.H., Byrne, P.M., Castro, G., Walberg, F.C., Perlea, V.G., Axtell, P.J., Dillon, J.C., Empson, W.B. and Mathews, D.L., 2012. Seismic deformation analysis of tuttle Creek dam. Canadian Geotechnical Journal, 49(3), 323-343.

Tichy M. (1994). First-order third-moment reliability method. Structural Safety, 16(3), 189-200.

Wang, L., Powers, M., Studiner, M., Fallatah, M., and Gong, W. (2018). Geotechnical Stability Analysis of Earthen Levees in the Face of Uncertainty. ASCE Geotechnical Special Publication 297, pp. 247-256.

Wang, L., Wu, C., Tang, L., Zhang, W., Lacasse, S., Liu, H., and Gao, L. (2020). Efficient reliability analysis of earth dam slope stability using extreme gradient boosting method. Acta Geotechnica, 15(11), 3135-3150.

Wang, W., Li, D.Q., Liu, Y., and Du, W. (2021). Influence of ground motion duration on the seismic performance of earth slopes based on numerical analysis. Soil Dynamics and Earthquake Engineering, 143, 106595.

Xiao, J., Gong, W., Martin II, J.R., Shen, M., and Luo, Z. (2016). Probabilistic seismic stability analysis of slope at a given site in a specified exposure time. Engineering Geology, 212, 53-62.

Zevenbergen, C., van Herk, S., and Rijke, J. (2017). Future-proofing flood risk management: Setting the stage for an integrative, adaptive, and synergistic approach. Public Works Management & Policy, 22(1), 49-54.

Zhang, J., Huang, H.W., and Phoon, K.K. (2013). Application of the Kriging-based response surface method to the system reliability of soil slopes. Journal of Geotechnical and Geoenvironmental Engineering, 139(4), 651-655.

Zhang, W.G., Wu, J.H., Gu, X., Han, L., and Wang, L. (2022). Probabilistic stability analysis of embankment slopes considering the spatial variability of soil properties and seismic randomness. Journal of Mountain Science, 19(5), 1464-1474.

Zhao, Y.G., and Ono, T. (2000). New point estimates for probability moments. Journal of Engineering Mechanics, 126(4), 433-436.

Zhao, Y.G., and Ono, T. (2001). Moment methods for structural reliability. Structural Safety, 23(1), 47-75.

List of Tables

List of Figures

Table 1. Geotechnical parameters for the earthen levee for deterministic analysis

Parameter	Foundation Soil	Embankment Soil	Rock Fill Zone	No. 57 Stone
Unit weight, kN/m^3	18.85	18.06	18.85	18.85
Secant stiffness in standard drained triaxial test, kN/m^2	20000	20000	30000	30000
Tangent stiffness for primary oedometer loading, kN/m^2	25610	25610	36010	36010
Unloading/reloading stiffness, kN/m^2	94840	94840	110800	110800
Power for stress-level dependency of stiffness	0.5	0.5	0.5	0.5
Effective cohesion, kN/m^2	1.2	1.2	1.2	0
Effective friction angle, °	32	30	30	36
Shear strain at which G_s= $0.722G_0$	0.00012	0.00012	0.00015	0.00015
Shear modulus at very small strains, kN/m^2	270000	270000	100000	100000
Poisson's ratio	0.2	0.2	0.2	0.2
Permeability coefficient, m/sec	0.000001	0.000001	0.00001	0.001

Table 2. Statistics of uncertain geotechnical parameters in probabilistic assessment (after Wang et al. 2018)

Uncertain Soil Parameter	Embankment Soil		Rockfill Zone		No. 57 Stone		Foundation Soil	
	Mean	COV	Mean	COV	Mean	COV	Mean	COV
Effective Cohesion (kN/m^2)	1.2	10%	1.2	10%	0	-	1.2	10%
Effective Friction Angle (°)	30	15%	30	10%	36	10%	32	15%
Permeability coefficient (m/sec)	1×10^{-6}	25%	1×10^{-5}	25%	1×10^{-3}	25%	1×10^{-6}	25%

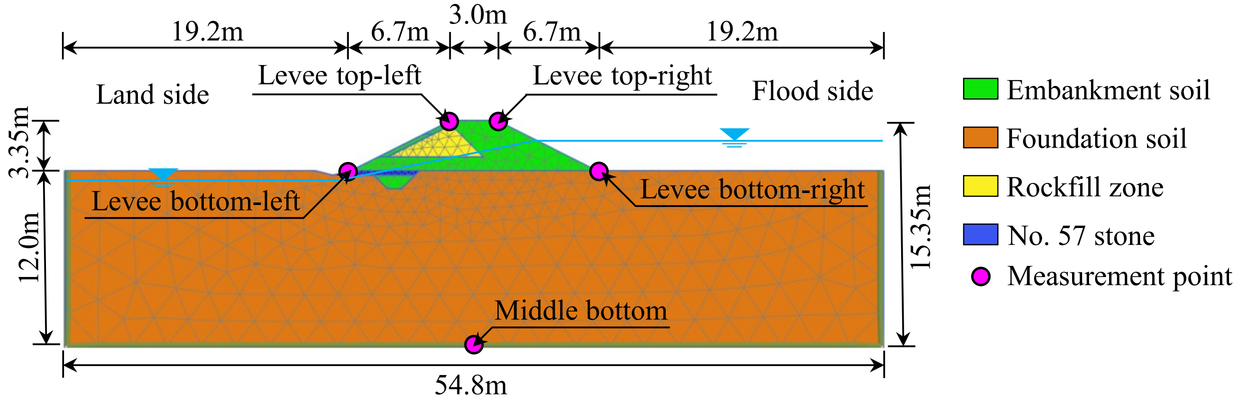

Figure 1: Illustration of the geometric layout of the earthen levee

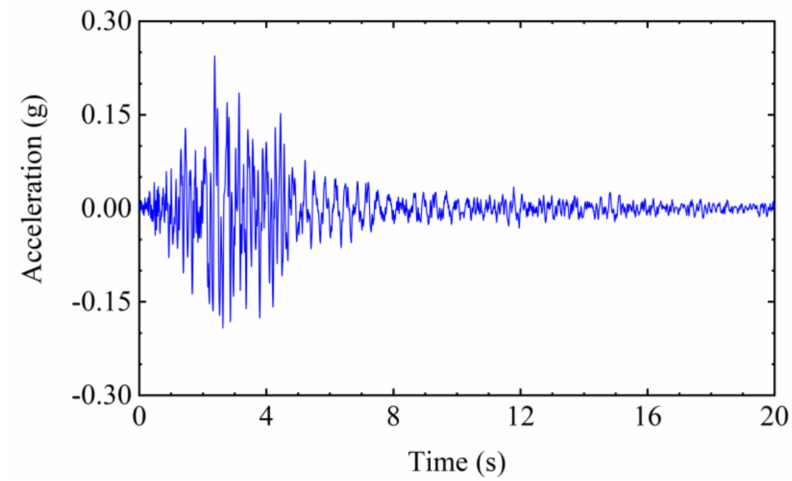

Figure 2. Acceleration time history of the input ground motion

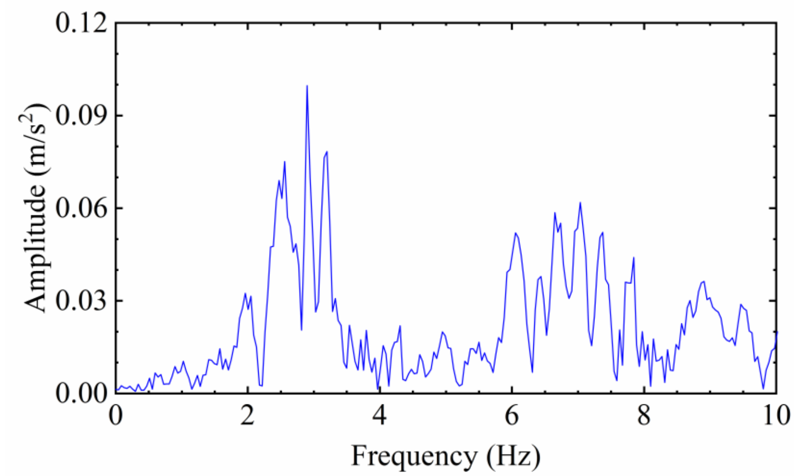

Figure 3. Fourier amplitude spectrum of the input ground motion

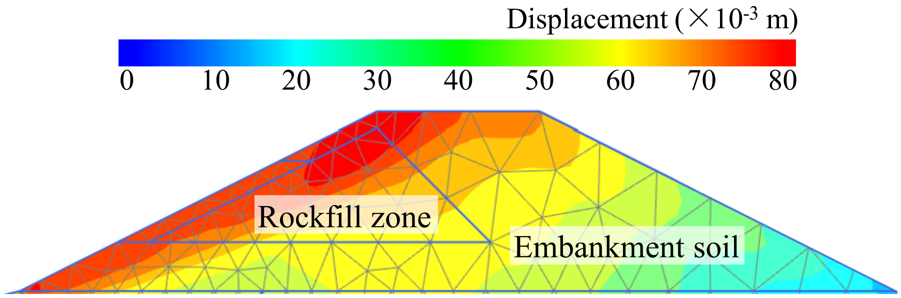

Figure 4. Contour plot of total permanent displacement of the levee at the end of shaking

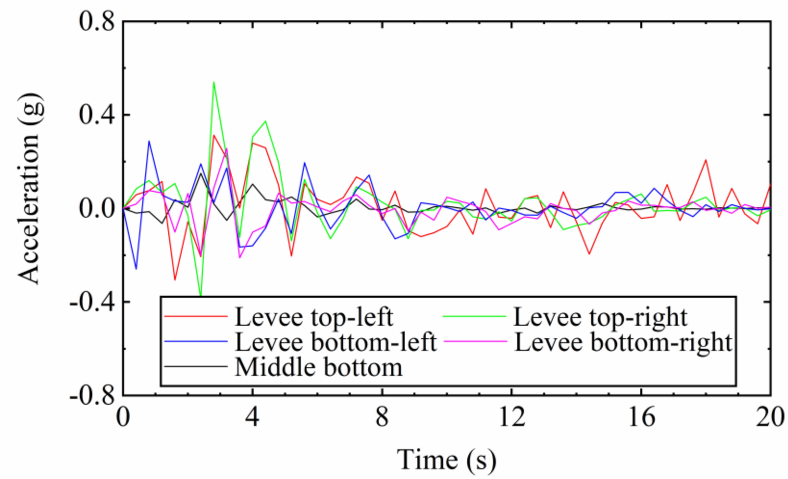

Figure 5. Horizontal acceleration time history on the five measurement points of the levee

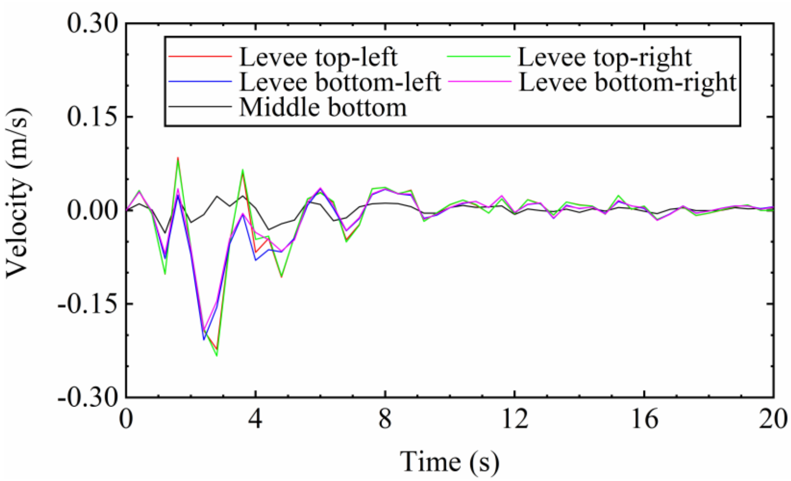

Figure 6. Horizontal velocity time history on the five measurement points of the levee

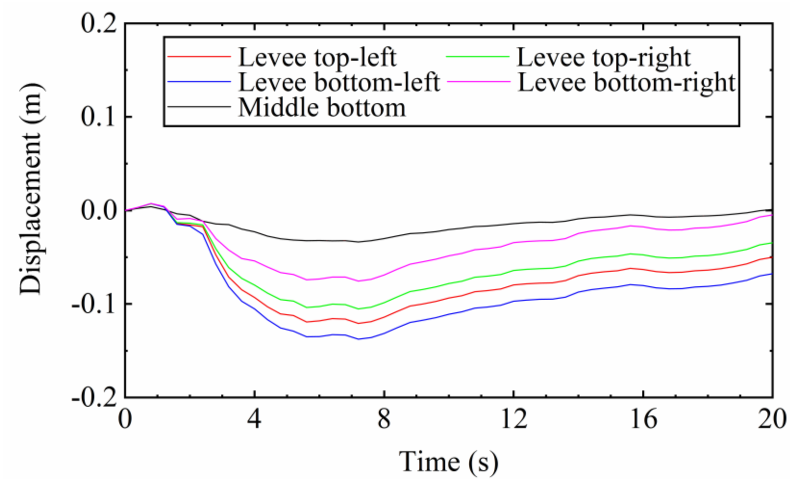

Figure 7. Horizontal displacement time history on the five measurement points of the levee

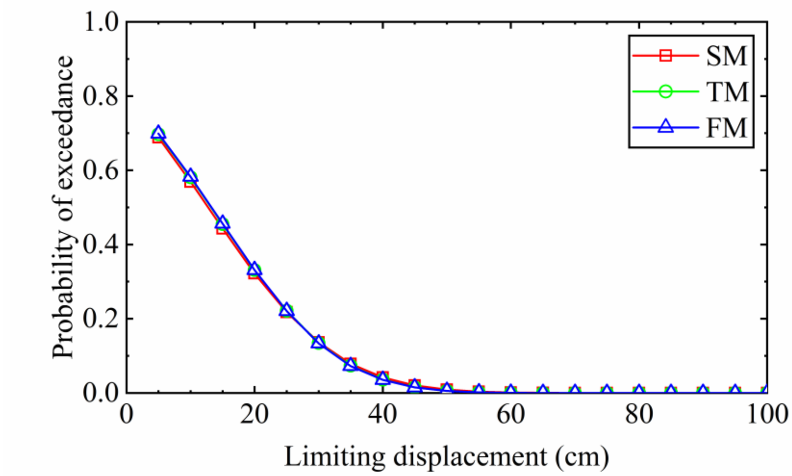

Figure 8. Probability of exceedance curves under the given earthquake load (PGA = 0.24 g) using different moment methods

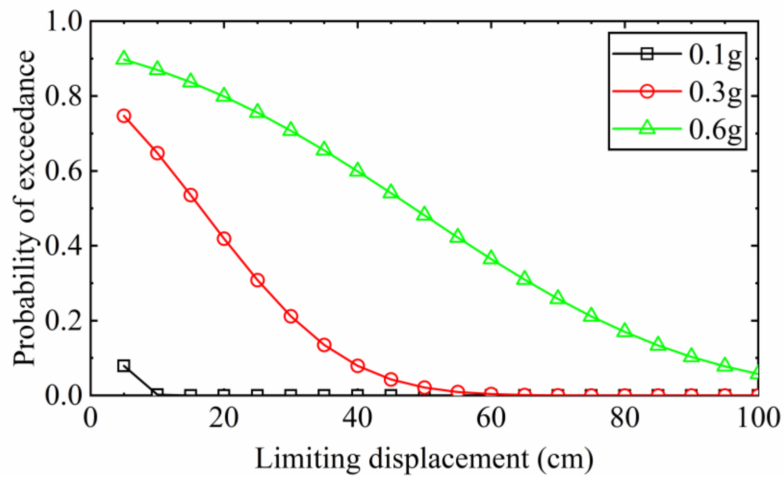

Figure 9. Probability of exceedance curve under different peak ground acceleration levels

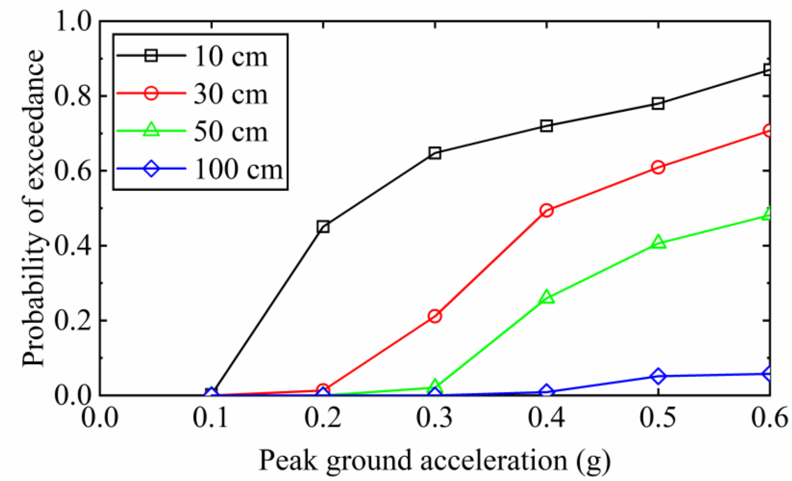

Figure 10. Effects of different limiting displacement values on the probability of exceedance versus the peak ground acceleration